Combining Different Reconstruction Kernel Responses as Preprocessing Step for Airway Tree Extraction in CT Scan

Samah Bouzidi[1,2], Fabien Baldacci[1], Chokri ben Amar[2] and Pascal Desbarats[1]
[1]*Univ. Bordeaux, LaBRI, UMR 5800, F-33400 Talence, France*
[2]*Research Group in Intelligent Machines (ReGIM), University of Sfax, Sfax, Tunisia*
{*sbouzidi, fabien.baldacci, pascal.desbarats*}*@u-bordeaux.fr, chokribenamar@ieee.org*

Keywords: Airway Tree Segmentation Pipeline, CT Reconstruction Kernels, Data Fusion, CT Chest Scan.

Abstract: In this paper, we propose a new preprocessing procedure that combines the responses of different Computed Tomography (CT) reconstruction kernels in order to improve the segmentation of the airway tree. These filters are available in all commercial CT scanner. A broad range of preprocessing techniques have been proposed but all of them operate on images reconstructed using a single reconstruction filter. In this work, the new preprocessing approach is based on a fusion of images reconstructed using different reconstruction kernels and can be included as a preprocessing stage in every segmentation pipeline. Our approach has been applied on various CT scans and an experimental comparison study between state of the art of segmentation approaches results performed on processed and unprocessed data has been made. Results show that the fusion process improves segmentation results and removes false positives.

1 INTRODUCTION

Lung disorders like asthma, chronic obstructive pulmonary disease, bronchiectasis and many more are associated with structural changes in airways. These deformations are characterized by a thickening of the airway walls and a narrowing of the airways lumen area. Therefore, the assessment and the treatment of such disorders require a good knowledge of airways morphology (Montaudon et al., 2007; Fetita et al., 1999). The diagnosis of the airways can be done by a direct observation of CT images. However, visual diagnosis is limited in practice because of the large number of slices under investigation. An accurate quantitative measurement of airway lumen dimension and wall thickness requires a (semi-) automatic segmentation of the airways tree.

Airway tree segmentation in CT images is a challenging task mainly due to the specific characteristics of the region of interest. Anatomically, an airway consists of a low-density lumenal area surrounded by high-density vascular airway wall (see Figure 2). The size of the wall and lumen decreases at each bifurcation (generation) as the tree is going deeper in the lung. Therefore, only airways located within generation $0-10$, having an average diameter that decrease from $15mm$ at the trachea to $1mm$ at the 10^{th} generation (Weibel and Gomez, 1962), can be imaged by current clinical CT scanners. Moreover, the tiny size of airways beyond the 6^{th} generation makes them less recognizable from the lung parenchyma.

Improvements in image resolution are usually accomplished by using thin slices which, however, expose the patient to high radiation dose or by interpolating additional slices (Aykac et al., 2003).

Besides of slice thickness parameter, radiologist can also adjust, during the reconstruction process, the reconstruction kernel which is usually chosen according to the studied organ.

Nevertheless, there has been no interest to investigate the effect of this parameter on the image quality. In this work, we propose to improve the quality of data by combining images obtained from more than a single reconstruction kernel. Merged volume is then employed as the input of any airways segmentation method.

In the literature, several airway tree segmentation methods have been proposed. For an overview of existing approaches we refer to the survey of (Pu et al., 2012) and (Lo et al., 2012). Mostly, proposed approaches are based on Region Growing (RG) algorithms. However, this technique deals with two main difficulties: it often leads to leakage into the lung parenchyma or stops earlier and gives an incomplete segmentation. Leakage occurs when the airway wall is obscured by noise and partial volume

Bouzidi S., Baldacci F., ben Amar C. and Desbarats P.
Combining Different Reconstruction Kernel Responses as Preprocessing Step for Airway Tree Extraction in CT Scan.
DOI: 10.5220/0006134200890097
In *Proceedings of the 12th International Joint Conference on Computer Vision, Imaging and Computer Graphics Theory and Applications (VISIGRAPP 2017)*, pages 89-97
ISBN: 978-989-758-225-7

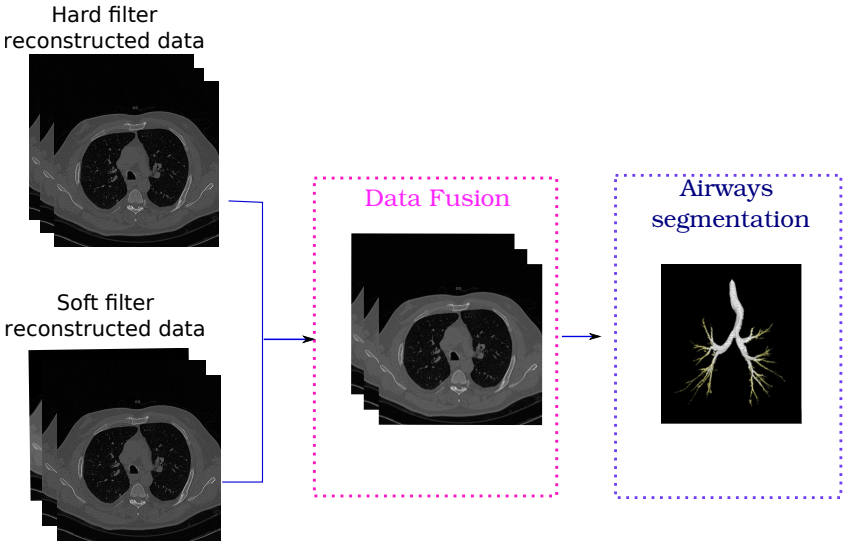

Figure 1: Overview of the segmentation pipeline.

effects. To overcome this problem, several strategies have been proposed. Adjusting the RG threshold iteratively and stopping the segmentation when leakage occurs are solutions proposed in (Mori et al., 1996; Kitasaka et al., 2003; Weinheimer et al., 2008). Other works address the RG leakage problem by filtering the image before performing the tree segmentation. In that approach, tubular enhancement filters based on hessian matrix analysis (Frangi et al., 1998; Sato et al., 1997; Krissian et al., 2000; Lo et al., 2009) and mathematical morphology operations (Aykac et al., 2003; Pisupati et al., 1996; Irving et al., 2009; Fabijańska, 2009) are used to isolate candidate airway locations. So far, and despite these efforts, none of these methods guarantee that the RG doesn't leak into lung parenchyma and that the full airway tree is constructed. In this paper, we combine CT volume reconstructed using different reconstruction kernels to create a new 3D image used as the input of airway segmentation pipelines. Data is reconstructed from the same CT acquisition therefore without exposing the patient to an additional radiation dose.
A quantitative and qualitative evaluation was conducted to assess the impact of the new data on the airways segmentation schemes in terms of the number of recognized bronchi and the rate of leakage. The content of this paper may be summarized as follows. In section 2, the proposed method is explained. Section 3 presents the experimental results and discusses the accuracy of the method. Finally, conclusions and perspectives are drawn in section 4.

2 METHOD

Our approach consists of introducing a new preprocessing step (Data fusion step) in the airway segmentation pipeline. An overview of the new segmentation pipeline is given by Figure 1. The inputs of the workflow, are two 3D X-ray CT volume reconstructed using soft and hard filters. We then apply, on the combined data, state of the art methods based on RG to extract the airways and reconstruct the tree.

2.1 Fusion of Reconstructed CT Volumes

In Computed Tomography scanning, cross-sectional images are reconstructed from the measurements of attenuation coefficients of the X-ray beams at different angles and positions. Besides the data acquisition efficiency, CT image quality greatly depends on the accuracy of the reconstruction process. During this operation, user intervention is limited to adjusting acquisition parameters such as the choice of the reconstruction kernel, also known as reconstruction filter.
There are several types of filters available in commercial CT scanners and the choice of the appropriate one depends on the explored organ.
In the case of CT lung exams, when data is reconstructed using a hard kernel, high-frequency components such as vessel and airway wall, pleura and sharp transitions are highlighted (see Figure 2.(a)). On the contrary, the soft kernel has the effect of filtering out high frequencies and letting low frequencies pass. Thus, this filter produces blurred images where noise

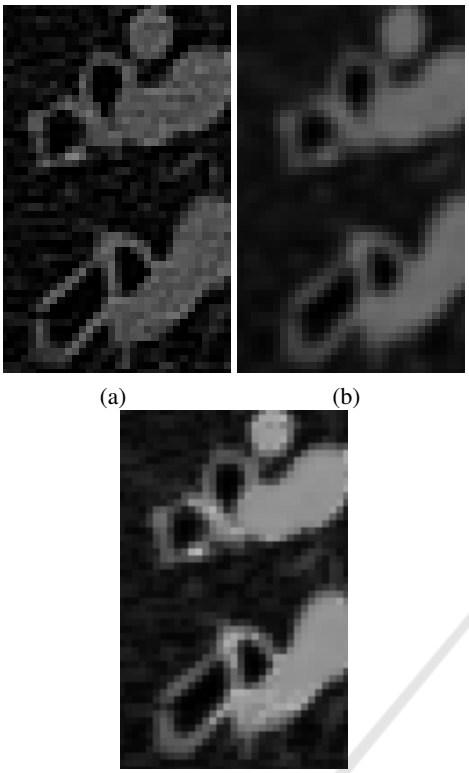

Figure 2: Three CT images reconstructed using (a) hard filter and (b) soft filter (c) the fusion of the data using soft and hard kernel. Airways appear in CT image as a dark structure surrounded by a bright and thin contour. Airways showed here belong to the 6^{th} generation.

is smoothed. However contours are attenuated (see Figure 2.(b)).
Most of airway tree segmentation algorithms based on RG try to retrieve and extract airway lumen pixels and then reconstruct the whole tree. Even if the airway wall pixels are not considered in the segmentation, they play a very important part in the growing process. In fact, The wall surrounds the lumen area, separates this region from the lung parenchyma and prevents the RG from leaking outside the airway lumen.

According to this constraint, it seems better to use the hard reconstruction kernel because it allows enhancing the airway wall contours. However, using this kernel thin contours are often obscured by noisy pixels. This leads to decrease the contrast between the air and the surrounding tissue. Then, the whole lung can be added to the growing region. Furthermore, if noisy pixels are located in airway lumen regions, growth can be interrupted earlier. Noise can be smoothed using the soft reconstruction kernel. However, using this filter, contours are smoothed too and airway lumen is narrowed, so the airway lumen cannot be well distinguished from the lung parenchyma and leakage can occurs or segmentation is stopped earlier.
In order to take advantages of each type of reconstruction, we propose to combine its resulting data in a single volume (see Figure 2.(c)) in which noise is smoothed and contours are enhanced. The fusion process can be added to any airways segmentation algorithm as a preprocessing step. Images are combined as follow:

$$I(x,y,z) = \begin{cases} I_{HF}(x,y,z) & \mid I_{HF}(x,y,z) \mid >= \mid I_{SF}(x,y,z) \mid \\ I_{SF}(x,y,z) & otherwise \end{cases}. \quad (1)$$

Where I_{HF} is the image reconstructed using the hard kernel and I_{SF} is the image reconstructed using the soft kernel. Considering that airway lumen are filled with air and have a very low and negative intensity in CT images. The combined volume takes from HF data high-intensity pixels (airway wall and vessel) and very low and negative intensity (airway lumen and parenchyma). Noise pixels, having high intensity, are replaced by smoothed one, having very low and negative intensity, given by the SF data.

2.2 Airways Tree Segmentation

In order to study the effect of the proposed fusion process, the airways segmentation stage has been performed using six state of the art algorithms. Furthermore, we have implemented a fast and simple RG algorithm to segment airways tree that we have also used for the assessment of the fusion procedure. These methods are:

- **Intensity based RG Approach.** (Mori et al., 1996) proposed a 3D "explosion-controlled" RG algorithm that starts from a seed placed inside the trachea. Adjacent voxels are added to the tree if their intensities are smaller than a threshold. The algorithm updates iteratively the intensity threshold until parenchymal leakage (explosion) is detected. The leakage is detected by comparing two successive segmentations. if the ratio between these segmentations is higher than an explosion control parameter, voxels added by the current threshold are removed and the algorithm is stopped. We have used this algorithm to automate all RG process proposed in the following approaches.
- **Multiscale Black Top-Hat based RG Approach.** In our previous work (Bouzidi et al.,

2016), we used a multiscale Black Top-Hat filter to enhance airways. The proposed airways enhancement filter aims to separate airways from adjacent lung parenchyma and vessels (see Figure 3). Based on the filter output, the RG is performed twice. First, an intensity based RG is applied to segment trachea and main bronchi (airways). Then, the input volume is enhanced using the multiscale Black Top-Hat filter. Thereafter, the second RG is performed on the processed volume to extract the airway tree and prevent leakage.

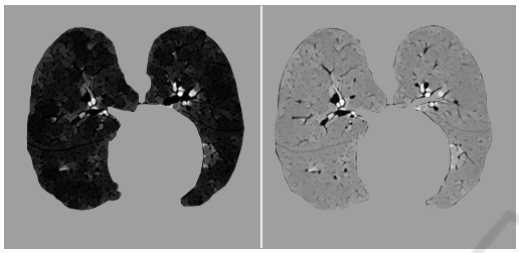

Figure 3: Airways highlighted using the Black Top-Hat transform. Left: the multiscale response of the filter applied in an axial slice. Right: its corresponding image difference.

- **Gradient based 3D RG Algorithm.** We propose here a very simple and fast algorithm to delineate the airways and then to reconstruct the airways tree. In this algorithm, we have applied the gradient operator in order to detect contours. The resulting volume contains vessel, airways and pleura contours. The volume contains also noisy pixels contours depending on the type of the input data (HF or SF data). Using the Otsu algorithm (Otsu, 1975), the gradient volume is thresholded. As the RG extract lumen regions, the interior of each contour is filled using a hole fill operator. Here, the interior of the pleura, the parenchyma, is excluded from the fill hole process. We then subtract from the obtained volume the thresholded gradient volume. This allows keeping only vessels and airways lumen but also some parenchyma pixels due to noise contours. All the pixels with density values in the initial volume lower than 900 HU (Hounsfield Units) are labeled as airway lumen since air has very low HU values around 1000 in CT slices, other pixels are removed from the volume. After that, The RG is performed to link airways lumen region of the processed volume in one final tree.
- **Mathematical Morphology based RG.** Mathematical morphology methods use a range of morphological structuring elements (SE) for the segmentation process. (Aykac et al., 2003) used grayscale mathematical morphology reconstruction to identify airways candidates on 2D CT slices. The grayscale reconstruction is performed using different sized SE in order to detect airways over a wide range of sizes. Airway tree is then reconstructed using a slice by slice RG algorithm.

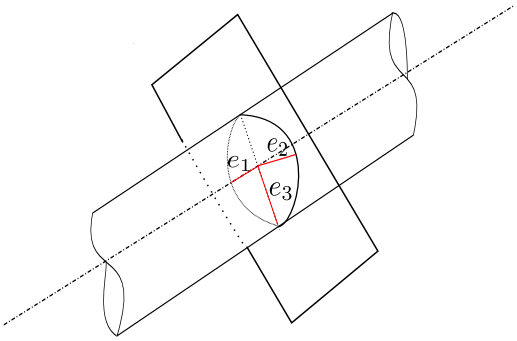

Figure 4: The eigenvalues e_2 and e_3 of the Hessian matrix define the principal curvature of the tube.

- **Hessian based RG Approaches.** The segmentation of tubular structures, which represent areas of lower intensity in the case of airways, can be achieved by studying the differential properties of the image and especially the analysis of the Hessian matrix of the image. In this field of research, a lot of tubular detection filters (Sato et al., 1997; Krissian et al., 2000; Frangi et al., 1998) have been proposed in the literature. Filters perform a shape analysis for each pixel in the image domain resulting in a kind of medialness or tube-likeliness measure. The extraction scheme, RG in our case, is then applied on the enhanced data to extract the whole tree. We will present here the theory behind vesselness filters.

Frangi Line Filter. (Frangi et al., 1998) perform a Hessian eigenvalue analysis to enhance voxel within tubular structures (vessels, airways...). Based on the information that dark tubular structures have two positive larger eigenvalues ($e_3 > 0$ *and* $e_2 > 0$) and the third eigenvalue being close to zero ($e_1 \approx 0$). The proposed line filter is defined as:

$$T(x) = \begin{cases} (1-exp(\frac{R_A^2}{2\alpha^2}))exp(\frac{R_B^2}{2\beta^2})(1-exp(\frac{S^2}{2\gamma^2})) \\ 0 \qquad\qquad\qquad\qquad e_3 < 0 \text{ and } e_2 < 0 \end{cases} \quad (2)$$

with $R_A = |\frac{e_2}{e_3}|$, $R_B = \frac{|e_1|}{\sqrt{e_2 e_3}}$ and S is the Frobenius norm of the Hessian matrix. α, β and γ are control parameters.

Sato Line Filter. Similar to the work of (Frangi et al., 1998). (Sato et al., 1997) proposed the

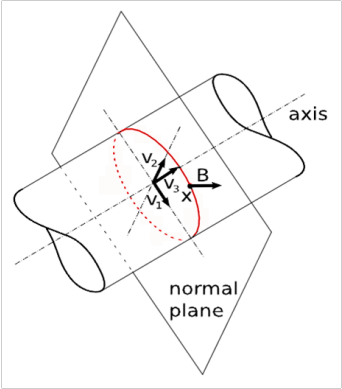

Figure 5: The medialness response obtained from the boundary information (red circle). The Cross-section plane of the tube is spanned by the eigenvectors v_1 and v_2 of the Hessian matrix.

following line filters to enhance tubular structures:

$$T(x) = \begin{cases} exp(-\frac{e_1^2}{2(\alpha_1 e_c)^2}) * e_c & e_1 \leq 0 \; and \; e_c \neq 0 \\ exp(-\frac{e_1^2}{2(\alpha_2 e_c)^2}) * e_c & e_1 > 0 \; and \; e_c \neq 0 \\ 0 & e_c = 0 \end{cases} \cdot \quad (3)$$

with $e_c = min(e_2, e_3)$, and α_1 and α_2 are control parameters.

Krissian Medialness Filter. Krissian et al. (Krissian et al., 2000) proposed a medialness function which measures the degree to belong to the medial axis. The response function is estimated by measuring the boundary information at a circular neighborhood which radius is the used scale. The proposed medialness function is represented as follows:

$$R(X, \sigma, \theta) = \frac{1}{N} \sum_{i=0}^{N-1} \mid \bigtriangledown I^{\sigma}(X + \theta \sigma v_{\alpha_i} \mid \quad (4)$$

Here, $X = (x, y, z)^T$ is a pixel point, $I^{\sigma}(X)$ is the image at the scale σ, N is the number of samples. The circle is defined by eigen vectors v_1 and v_2 and the radius $r = \sigma\theta$.

3 EXPERIMENTS AND RESULTS

The performance of the proposed approach in terms of filter responses (Frangi et al., 1998; Sato et al., 1997; Krissian et al., 2000; Aykac et al., 2003; Bouzidi et al., 2016) and segmentation results has been qualitatively and quantitatively compared to those obtained when the input of the segmentation pipeline is only one type of reconstructed data. We have compared the results of combined data to the results of SF data because lung CT data are usually reconstructed using SF kernel and airways tree obtained from the HF data leaks to the lung parenchyma (see Figure 6).

Table 1: Description of the dataset.

Scan	Spacing (mm)	Z-spacing (mm)	number of slices	kV/mAs
01	0.67	1	306	120/155
02	0.71	1	272	120/128
03	0.65	1	286	120/152
04	0.74	1	344	120/152
05	0.74	1	304	120/155
06	0.63	1	323	120/155
07	0.57	1	300	120/152
08	0.68	1	319	120/152
09	0.7	1	300	120/158
10	0.72	1	286	120/152
11	0.7	1	300	120/152
12	0.71	1	300	120/155

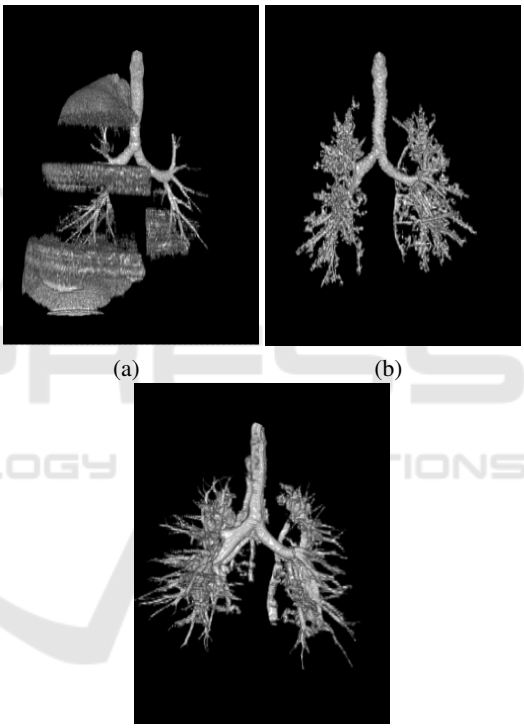

(a) (b)

(c)

Figure 6: Airway tree segmentations using the HF data. (a) (Aykac et al., 2003). (b) Gradient based method (c) (Bouzidi et al., 2016).

We applied our method to twelve CT chest scan available in two examples: images reconstructed using the hard kernel and images reconstructed using the soft kernel. Table 1 presents the characteristics of each scan. All computations were performed on an intel-Xeon E3-1200 @3.60GHz, 16GB RAM, Ubuntu Linux 64 bit.

We first investigate the impact of the combined data on Hessian based (Frangi et al., 1998; Sato et al., 1997; Krissian et al., 2000) and morphological based (Aykac et al., 2003; Bouzidi et al., 2016) airways filter responses. Figure 7 reports filters responses of (Aykac et al., 2003) (Figure 7.(a)) and (Frangi et al., 1998) (Figure 7.(b)) on the SF data (left side) and combined data (right side). In (Aykac et al., 2003) and (Bouzidi et al., 2016) segmentation approaches, the fusion of HF and SF data has an effect of noise reduction, as can be seen in Figure 7.(a), especially before the first bifurcation of the tree. This can be explained by the improvement of the contrast between airway lumen and parenchyma given by the hard reconstruction. Such improvement allows the employed morphological operator (Black Top-Hat operator, grayscale closing reconstruction respectively) to enhance only grayscale minima corresponding to candidate airway locations and remove false positives (parenchyma pixels). Similarly, (Frangi et al., 1998)'s filter succeeds to enhance more airways when it is employed on combined data (see Figure 7.(b)). As a consequence, the improvement in filters responses of the combined data will guide and constraint the segmentation process to retrieve more enhanced bronchi without leaking into parenchyma. An example of segmentations using (Aykac et al., 2003) approach is shown in Figure 8. Leakages that occur in the segmentation based on the SF data are excluded when we use the combined data. Further, more deeper airways has been added to the tree. The branch detection number for each method and data will be detailed in Table 2.

We then compare all segmentation results in terms of tree depth (number of retrieved generation) and the number of retrieved bronchi per generation. Using these two metrics, we compare for each method airway trees obtained from combined data and SF data. An example of the combined data effect on the gradient based 3D RG is shown in Figure 9. The airway tree extracted from the HF data (Figure 9.(a)) presents a very high rate of false positives (parenchyma voxels misclassified as lumen area voxels). The airway tree extracted from the SF data reached only the 4^{th} generation while the merged data allows to extend the segmentation to the 10^{th} generation.

Quantitative improvement of the data fusion on the segmentation results is given in Table 2 and Table 3. In Table 2, we give for each scan the total number of extracted bronchi from the processed and unprocessed data (SF reconstructed data) and we detail in Table 3 the maximum, minimum and the average of retrieved airways per generation in all the dataset. We limit our investigation to recognized bronchi from the 4^{th} to 7^{th} generation because, first, all methods successfully extract all airways until the four first generation. Second, beyond the 7^{th} generation, methods, whatever the input data, fail to identify more than an average of five airways, which cannot be used in practice. For that reason alsov, we didn't give in table 3 the statistics of detected bronchi at these generations.

Table 2 shows that (Aykac et al., 2003), (Bouzidi et al., 2016) and the gradient based method has more

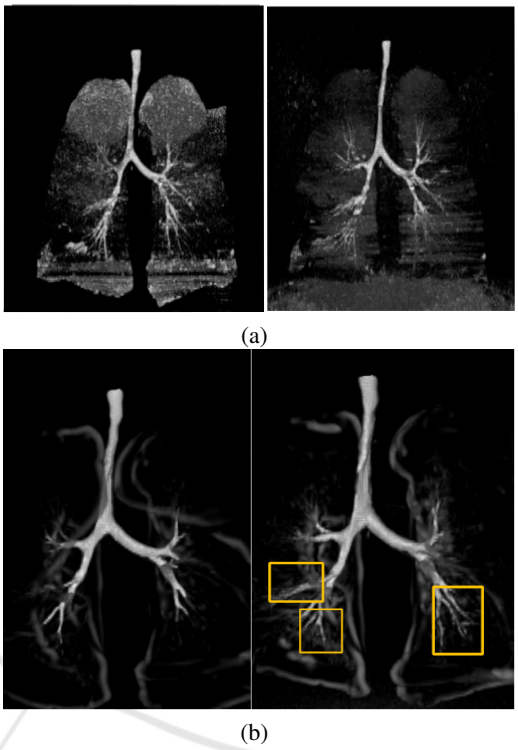

(a)

(b)

Figure 7: Aykac and Frangi filter responses when the data is combined (right) or not (left). (a) Aykac's filter responses. (b) Frangi's filter responses. In Aykac's filter, the combined data has an effect of noise remover. In Frangi's filter, new enhanced airways are marked in yellow rectangle.

Figure 8: Airways tree segmentations using the method of (Aykac et al., 2003) applied on the SF reconstructed data (in the left) and on the merged data (in the right). The combined data allows to remove the leakage that occurs in the segmentation of the SF data.

Table 2: Comparison of the number of recognized bronchi using SF reconstructed data (SF data) and combined data (C data) over 12 human CT scans. gray cell : leakage occurs in the segmentation, G: gradient based algorithm, TH: Top-Hat based algorithm, AY: Aykac algorithm, FR: Frangi based algorithm, SA: Sato based algorithm, KR: Krissian based algorithm.

	G		**TH**		**AY**		**FR**		**SA**		**KR**	
	SF data	C data	SF data	C data	SF data	C data	SF data	C data	SF data	C data	SF data	C data
Scan1	33	52	43	63	76	82	37	41	31	33	33	36
Scan2	20	67	47	67	62	72	32	34	26	30	23	26
Scan3	7	76	37	62	76	84	35	35	29	31	25	25
Scan4	15	34	27	43	52	58	27	32	25	27	17	17
Scan5	16	58	44	60	66	72	28	28	26	26	17	17
Scan6	7	52	39	65	61	80	35	35	29	29	31	35
Scan7	45	60	47	90	63	75	30	33	27	29	24	25
Scan8	37	50	45	56	55	60	31	35	26	30	15	17
Scan9	28	42	35	47	41	49	24	27	24	24	22	22
Scan10	25	76	60	84	75	85	27	29	25	25	25	25
Scan11	31	82	41	82	65	68	20	22	27	30	21	21
Scan12	32	54	43	60	59	68	33	38	33	36	25	27
Min gain	13		11		3		0		0		0	
Max gain	69		43		20		5		4		4	
Avreage	33.92		22.58		10		2.5		1.83		1.25	

Table 3: Maximum, minimum and avreage of airways detection as a function of apparent generation. Trachea is the generation zero. m :minimum of detected airways, M :maximum of detected airways, μ: Average of detected airways, G: gradient based algorithm, TH: Top-Hat based algorithm, AY: Aykac algorithm, FR: Frangi based algorithm, SA: Sato based algorithm, KR: Krissian based algorithm.

Apparent Generation		4			5			6			7		
		m	M	μ	m	M	μ	m	M	μ	m	M	μ
G	SF data	0	14	6.58	0	11	3.25	0	4	0.67	0	2	0.17
	C data	11	21	16.17	3	24	13.8	2	15	6.92	0	8	6
TH	SF data	10	21	14.2	2	20	8.33	0	8	2.17	0	2	0.83
	C data	14	20	16.4	4	24	14.8	2	22	9.08	0	12	3.45
AY	SF data	10	19	15	6	22	16	4	16	9.8	0	10	5
	C data	10	20	16	10	24	17.5	6	18	13.4	0	13	6
FR	SF data	4	14	9.3	2	8	3	0	6	2.17	0	2	0.33
	C data	5	14	10.41	2	9	4	0	6	2.17	0	2	0.33
SA	SF data	6	12	8.83	2	6	2.5	0	2	0.67	0	0	0
	C data	6	12	9.75	2	9	3.08	0	2	0.67	0	0	0
KR	SF data	0	10	6.3	0	2	1.2	0	6	0.7	0	0	0
	C data	2	12	7.08	0	3	1.25	0	6	0.67	0	2	0.16

benefited from the use of the combined data than Hessian based segmentation methods. These methods extract new branches that were missing from the SF data reconstructed data. For example, for the second scan and using the combined data (Aykac et al., 2003), (Bouzidi et al., 2016) and the gradient based method add respectively 10, 20 and 40 new airways to the trees obtained from the SF data. This leads to add 1-3 extra generations of airway branches. We summarize in Table 4 gains in term of added bronchi of each method over the dataset. A slight improvement, less than five added bronchi, is associated to Hessian based segmentation results even though the prominent improvement of their filters responses using the output of the fusion step. This behaviour is due to the lack of direction information, given by these filters to retrieve tubular structures (airways in our case), in the RG algorithm. Further, the proposed preprocessing step has allowed preventing the RG from leakage produced when the input is the SF data. We specify in Table 2 (gray cell) segmentations where the leakage occur. Note that airways which are recognized after the leakage are not considered in the final tree.

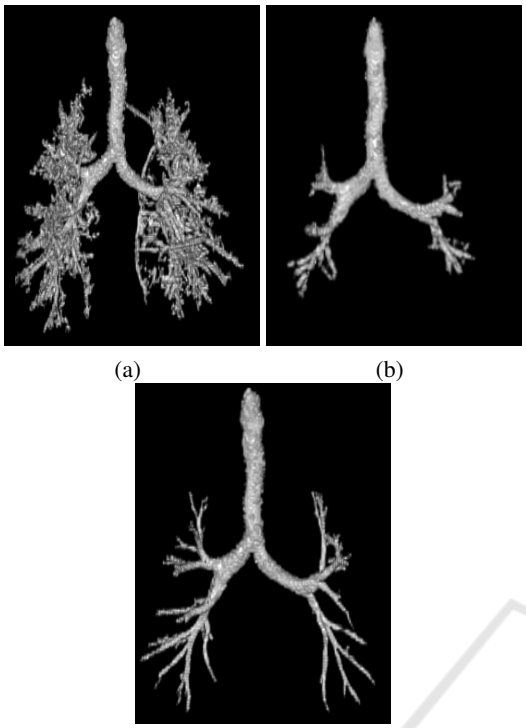

(a) (b)

(c)

Figure 9: Comparison of airway tree segmentations produced by the gradient based RG using the creterion of (Mori et al., 1996) on the third CT exam. (a) The *HF tree* contains leakage caused by parenchyma voxels misclassified as air voxels. (b) Leakage doesn't occur in the *SF tree* but the segmentation is stopped earlier (c) Obtained tree when the SF data is combined with the HF data. the tree penetrates deeper into the lung without leaking into the parenchyma.

Table 4: Overall gains in term of added bronchi of the segmentation methods over 12 human CT scans. G: gradient based algorithm, TH: Top-Hat based algorithm, AY: Aykac algorithm, FR: Frangi based algorithm, SA: Sato based algorithm, KR: Krissian based algorithm.

	Minimal gain	**Maximal gain**	**Avreage**
TH	11	43	22.58
G	13	69	33.92
A	3	20	10
FR	0	5	2.5
SA	0	4	1.83
KR	0	4	1.25

4 CONCLUSION AND PERSPECTIVES

In this paper, we have proposed a new preprocessing procedure that can be incorporated in any airways segmentation process. The idea behind this method is combining responses of different reconstruction kernels, available in all commercial CT scan. Data is reconstructed from the same acquisition so without exposing the patient to additional radiation dose. Combined data shows good results in terms of the number of recognized bronchi and the rate of leakage. Future works will focus on combining more than two reconstruction kernels responses and assessing its impact in the segmentation schemes. In our case, we have used two reconstruction kernel response : HF data and SF data. The first allows enhancing airway wall contours and the second, the standard data used in the airway segmentation task, smooths noisy pixels.
Furthermore, we plan to adapt and test the proposed procedure to segment other lung structures (vessels, nodules...).

ACKNOWLEDGEMENTS

The authors would like to thank radiologists from University Hospital Centre of Bordeaux Haut-Lévêque for providing lung CT images.

REFERENCES

Aykac, D., Hoffman, E. A., McLennan, G., and Reinhardt, J. M. (2003). Segmentation and analysis of the human airway tree from three-dimensional x-ray CT images. *Medical Imaging, IEEE Transactions on*, 22(8):940–950.

Bouzidi, S., Baldacci, F., Amar, C. B., and Desbarats, P. (2016). 3D segmentation of the tracheobronchial tree using multiscale morphology enhancement filter. In *Proc. of 24th International Conference on Computer Graphics, Visualization and Computer Vision*, pages 207–214.

Fabijańska, A. (2009). Two-pass region growing algorithm for segmenting airway tree from MDCT chest scans. *Computerized Medical Imaging and Graphics*, 33(7):537–546.

Fetita, C. I., Grenier, P., et al. (1999). Modeling, segmentation, and caliber estimation of bronchi in high resolution computerized tomography. *Journal of Electronic Imaging*, 8(1):36–45.

Frangi, A. F., Niessen, W. J., Vincken, K. L., and Viergever, M. A. (1998). Multiscale vessel enhancement filtering. In *Medical Image Computing and Computer-Assisted Interventation MICCAI98*, pages 130–137. Springer.

Irving, B., Taylor, P., and Todd-Pokropek, A. (2009). 3D segmentation of the airway tree using a morphology based method. In *Proceedings of 2nd international workshop on pulmonary image analysis*, pages 297–07.

Kitasaka, T., Mori, K., Suenaga, Y., Hasegawa, J.-i., and Toriwaki, J.-i. (2003). A method for segmenting bronchial trees from 3Dchest x-ray ct images. In *International Conference on Medical Image Computing and Computer-Assisted Intervention*, pages 603–610. Springer.

Krissian, K., Malandain, G., Ayache, N., Vaillant, R., and Trousset, Y. (2000). Model-based detection of tubular structures in 3D images. *Computer vision and image understanding*, 80(2):130–171.

Lo, P., Sporring, J., Pedersen, J. J. H., and de Bruijne, M. (2009). Airway tree extraction with locally optimal paths. In *Medical Image Computing and Computer-Assisted Intervention, MICCAI 2009*, pages 51–58. Springer.

Lo, P., Van Ginneken, B., Reinhardt, J. M., Yavarna, T., De Jong, P. A., Irving, B., Fetita, C., Ortner, M., Pinho, R., Sijbers, J., et al. (2012). Extraction of airways from CT (exact'09). *Medical Imaging, IEEE Transactions on*, 31(11):2093–2107.

Montaudon, M., Desbarats, P., Berger, P., De Dietrich, G., Marthan, R., and Laurent, F. (2007). Assessment of bronchial wall thickness and lumen diameter in human adults using multi-detector computed tomography: comparison with theoretical models. *Journal of anatomy*, 211(5):579–588.

Mori, K., Hasegawa, J.-i., Toriwaki, J.-i., Anno, H., and Katada, K. (1996). Recognition of bronchus in three-dimensional x-ray CT images with applications to virtualized bronchoscopy system. In *Pattern Recognition, 1996., Proceedings of the 13th International Conference on*, volume 3, pages 528–532. IEEE.

Otsu, N. (1975). A threshold selection method from gray-level histograms. *Automatica*, 11(285-296):23–27.

Pisupati, C., Wolff, L., Zerhouni, E., and Mitzner, W. (1996). Segmentation of 3D pulmonary trees using mathematical morphology. In *Mathematical morphology and its applications to image and signal processing*, pages 409–416. Springer.

Pu, J., Gu, S., Liu, S., Zhu, S., Wilson, D., Siegfried, J. M., and Gur, D. (2012). CT based computerized identification and analysis of human airways: a review. *Medical physics*, 39(5):2603–2616.

Sato, Y., Nakajima, S., Atsumi, H., Koller, T., Gerig, G., Yoshida, S., and Kikinis, R. (1997). 3D multi-scale line filter for segmentation and visualization of curvilinear structures in medical images. In *CVRMed-MRCAS'97*, pages 213–222. Springer.

Weibel, E. R. and Gomez, D. M. (1962). Architecture of the human lung. *Science*, 137(3530):577–585.

Weinheimer, O., Achenbach, T., and Düber, C. (2008). Fully automated extraction of airways from CT scans based on self-adapting region growing. *Computerized Tomography*, 27(1):64–74.